Multiple Spectral Peak Tracking for Heart Rate Monitoring from Photoplethysmography Signal During Intensive Physical Exercise

Navaneet K. Lakshminarasimha Murthy, Pavan C. Madhusudana, Pradyumna Suresha, Vijitha Periyasamy, and Prasanta Kumar Ghosh, *Senior Member, IEEE*

***Abstract*—We propose a multiple initialization based spectral peak tracking (MISPT) technique for heart rate monitoring from photoplethysmography (PPG) signal. MISPT is applied on the PPG signal after removing the motion artifact using an adaptive noise cancellation filter. MISPT yields several estimates of the heart rate trajectory from the spectrogram of the denoised PPG signal which are finally combined using a novel measure called trajectory strength. Multiple initializations help in correcting erroneous heart rate trajectories unlike the typical SPT which uses only single initialization. Experiments on the PPG data from 12 subjects recorded during intensive physical exercise show that the MISPT based heart rate monitoring indeed yields a better heart rate estimate compared to the SPT with single initialization. On the 12 datasets MISPT results in an average absolute error of 1.11 BPM which is lower than 1.28 BPM obtained by the state-of-the-art online heart rate monitoring algorithm.**

***Index Terms*—Adaptive noise cancellation, heart rate monitoring, spectral peak tracking.**

I. Introduction

REAL-TIME heart rate (HR) estimation from the photoplethysmography (PPG) signal is a key step in developing wearable devices that can monitor the HR in a non-invasive way [1], [2]. The PPG signal is optically obtained by pulse oximeters and its periodicity corresponds to the cardiac rhythm [3]. In spite of the HR information available in the PPG signal, reliable estimation of the HR is not straight-forward due to the fact that the PPG signal is vulnerable to motion artifacts (MA), which strongly interfere with the HR. Given that such wearable devices are widely used by field medics and during sports activity, depending on the type of physical activity of the user, the MA component can completely mask the HR information in the PPG signal causing the HR monitoring from the PPG signal challenging [4], [5].

A typical approach in estimating the HR in the presence of MA is to first remove MA from the PPG signal. There are several techniques in the literature for removing MA from the PPG signal [6]. A few denoising techniques do not require motion data [7] from an accelerometer while some others do. Independent Component Analysis (ICA) is one technique where motion data is not required; however, it requires multiple PPG sensors [8]. ICA has been proposed in both time-domain [9] and frequency-domain [10]. However, the assumption of statistical independence in ICA does not hold well in the PPG signal contaminated by MA [11].

On the other hand, when the acceleration data is available, the MA component is adaptively canceled from the PPG signal using adaptive filter based algorithms including least mean square (LMS), normalized LMS [12], [13], fast transversal recursive least square (RLS) [14] algorithms as well as spectrum subtraction technique [15] and Laguerre basis function based signal representation [16]. Other MA-removal techniques include physical artifact model [17], time-frequency analysis [18], wavelet denoising [19], [20], higher order statistics [10] and empirical mode decomposition [21], [22], to name a few. However, in case of an intensive physical exercise, most of these techniques do not work well [11]. Acceleration data has also been used for the observation model of Kalman filter [23] as well as Kalman smoother [24] to remove MA.

In contrast to the adaptive filtering [25], Zhang *et al.* [11] proposed a TROIKA framework, where a high-resolution spectrum of the PPG signal is calculated using sparse signal reconstruction following signal decomposition using the singular spectrum analysis. Spectral peak tracking (SPT) is performed on the reconstructed PPG spectra to estimate the HR, which has been shown to be effective when there is a strong MA component in the PPG signal. However, the SPT solely depends on the initialization of the HR in the first frame. In case of erroneous initialization, the entire estimated HR trajectory could be different from the actual HR trajectory.

In another approach, namely JOSS, proposed by Zhilin Zhang [26], common spectral structures between the PPG signal and the accelerometer signals are exploited. Multiple measurement vector model is used for joint sparse spectrum reconstruction. To remove the frequency bins of MA in the PPG spectrum, spectral

Manuscript received April 06, 2015; revised August 26, 2015; accepted September 27, 2015. Date of publication October 05, 2015; date of current version October 13, 2015. The associate editor coordinating the review of this manuscript and approving it for publication was Prof. Peng Qiu.

N. K. Lakshminarasimha Murthy, P. C. Madhusudana, P. B. Suresha are with National Institute of Technology, Surathkal, Mangalore-575025, Karnataka, India (e-mail: klnavaneet@ieee.org; pavancm@ieee.org; pradyumnaiyer21@ieee.org).

V. Periyasamy was with the Department of Electrical Engineering, Indian Institute of Science, Karnataka, Bangalore-560012, India. She is now with the School of Chemical and Biomedical Engineering, Nanyang Technological University, 637459 Singapore (e-mail: vijitha.periyasamy.in@ieee.org).

P. K. Ghosh is with the Department of Electrical Engineering, Indian Institute of Science, Karnataka, Bangalore-560012, India (e-mail: prasantg@ee.iisc.ernet.in).

Color versions of one or more of the figures in this paper are available online at http://ieeexplore.ieee.org.

Digital Object Identifier 10.1109/LSP.2015.2486681

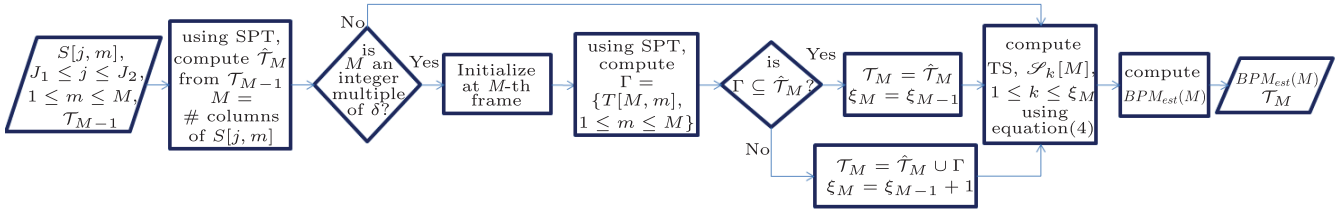

Fig. 1. Flowchart for the MISPT based HR estimation at the M-th frame. Along with the HR estimate, $\mathcal{T}_M$ is returned for an input in the next frame.

subtraction is performed on the reconstructed spectrum. SPT is similar to that in the TROIKA framework [11] with a trigger of discovery mechanism whenever the estimated HR does not change for three consecutive frames.

Among different available MA cancellation algorithms, we, in this work, choose Windrow's adaptive noise cancellation (ANC) [27], which was used to remove in-band motion disturbances in the PPG signal [28]. In order to estimate the HR from the denoised PPG signal, we perform SPT in a manner similar to the work by Zhang *et al.* [11], [26]. However, we include a novel multiple initialization scheme unlike single initialization in TROIKA [19] or a trigger-driven initialization in JOSS [26]. We refer to the proposed approach as multiple initialization based SPT (MISPT), in which multiple estimated HR trajectories from multiple initializations are combined using a novel measure called trajectory strength. We demonstrate the benefit of multiple initializations by estimating HR from the PPG signal recorded during intensive physical exercise.

We begin with a detailed description of the MISPT based HR estimation in the next section (Section II). In Section III, we summarize the results on the 12 datasets which are used in [26]. We experimentally show that multiple initializations indeed help in obtaining better HR estimates compared to single initialization. Conclusions are made in Section IV.

II. MISPT Based HR Estimation

MISPT based HR estimation consists of two stages, which are described in detail in the following subsections.

A. MA Removal

MA removal using ANC is the first step in the proposed MISPT based HR estimation. In ANC [28], a linear model is assumed for deriving a relation between the motion and the corresponding artifact in the PPG signal. In other words, the artifact $w[n]$ is related to the motion $a[n]$ through a linear filter $h[n]$ i.e., $w[n] = h[n]*a[n]$ where $*$ denotes the convolution operator. For computational convenience, we approximate the filter to have an impulse response of finite order. We also assume that the MA is additive, i.e., the observed PPG signal $y[n] = y_0[n] + w[n]$, where $y_0[n]$ is the original PPG signal.

Given these assumptions, we try to recover $y_0[n]$ by estimating $h[n]$. The cost function to be minimized by the filter is the mean squared error between $y[n]$ and $y_0[n]$ [16]. $h[n]$ is assumed to be adaptive in that its coefficients change for every analysis window.

The estimated filter with the impulse response $h'[n]$ gives us the estimated MA, $w'[n]$, as:

$$w'[n] = h'[n]*a[n] \tag{1}$$

The denoised PPG signal, $\hat{y}_0[n]$, is then estimated as:

$$\hat{y}_0[n] = y[n] - w'[n] \tag{2}$$

For estimation of HR, spectrum of $\hat{y}_0[n]$ is computed using the fast Fourier transform with an order $NFFT$.

B. Multiple Initialization Spectral Peak Tracking

MISPT is the second step in the proposed approach. In MISPT, the HR estimate at the M-th frame is obtained using spectra of all frames till the M-th frame, i.e., $S[j,m]$, $J_1 \le j \le J_2$ and $1 \le m \le M$, where J_1 and J_2 are frequency location indices corresponding to 0.4 and 5 Hz respectively. These frequencies are chosen because the HR typically lies within the range 0.4-5 Hz. $S[j,m]$ denotes the spectrum of $\hat{y}_0[n]$ at the j-th frequency bin at the m-th frame. Typically the location corresponding to the highest peak in the spectrum of a frame reflects the HR at that frame.

However, the peak corresponding to the HR may be masked when there is a strong or overlapping MA component. In such scenarios, SPT [11] is generally performed to estimate HR over frames (HR trajectory).

Unlike the traditional SPT, in the proposed MISPT, the initialization is done at every δ frame(s) starting with the first frame. If initialization is done at η-th frame, the SPT is performed in both forward and backward directions to obtain a HR trajectory denoted by $T[\eta,m]$, $1 \le m \le M$ and $\eta = 1, \delta+1, 2\delta+1, \cdots$. Since a HR trajectory is initiated at every δ frame, $\lfloor \frac{M}{\delta} \rfloor$[1] HR trajectories would be present at the M-th frame. However, many of these trajectories may be identical to each other. Let $\hat{T}_k[m], 1 \le m \le M, 1 \le k \le \xi_M$ be the k-th unique HR trajectory at the M-th frame where ξ_M is the number of unique trajectories. Let the set of unique HR trajectories at the M-th frame be denoted by

$$\mathcal{T}_M = \left\{ \hat{T}_k[m], 1 \le m \le M, 1 \le k \le \xi_M \right\}. \tag{3}$$

The HR is finally estimated using a measure called trajectory strength (TS) of the unique trajectories in $\mathcal{T}_M$. The flowchart (Fig. 1) illustrates the steps involved in MISPT at the M-th frame. In order to reduce the computational complexity in MISPT implementation, $\mathcal{T}_M$ is computed in a recursive manner, i.e., $\mathcal{T}_{M-1}$ is used as an input in addition to the denoised spectrogram up to the M-th frame. The details of the SPT and the TS based HR estimation are explained in the following subsections.

1) SPT: Both forward and backward SPT on the denoised PPG spectrogram are done in a manner similar to the algorithm

[1] $\lfloor x \rfloor$ denotes the highest integer less than x.

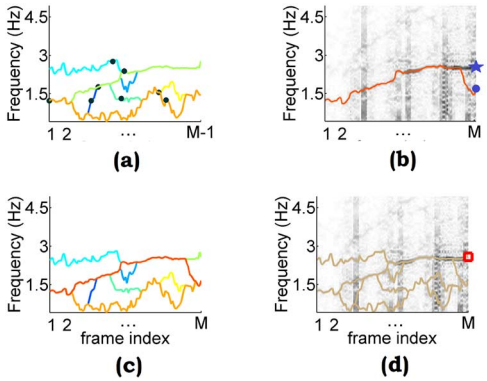

Fig. 2. Illustration of MISPT based HR estimation at M-th frame - (a) $\mathcal{T}_{M-1}$, unique trajectories till $(M-1)$-th frame, (b) $\Gamma = \{T[M,m], 1 \le m \le M\}$, trajectory initialized at M-th frame (c) $\mathcal{T}_M$, (d) Estimated HR.

proposed by Zhang *et al.* [11] involving three main steps - initialization, peak selection, and verification. The search range for the peak in the current frame is set around the peak location of the neighboring frame using a small positive integer Δ_s.

As shown in Fig. 1, at first the SPT is performed on the unique trajectories in $\mathcal{T}_{M-1}$ using the spectrum of the M-th frame to obtain $\hat{\mathcal{T}}_M = \{\hat{T}_k[m], 1 \le m \le M, 1 \le k \le \xi_{M-1}\}$. If the current frame (M) is an integer multiple of δ, then the spectral initialization followed by the backward SPT is executed to get a new trajectory Γ of length M. If this new trajectory (Γ) matches exactly with any of the unique trajectories from $\hat{\mathcal{T}}_M$, then $\hat{\mathcal{T}}_M$ is assigned to $\mathcal{T}_M$. Otherwise the union of Γ and $\hat{\mathcal{T}}_M$ is assigned to $\mathcal{T}_M$. This increments the number of unique trajectories by one.

2) TS Based HR Estimation: Due to MISPT, we obtain ξ_M unique trajectories at the M-th (current) frame. Let us denote the TS of the k-th unique trajectory by $\mathsf{S}_k[M]$ defined as

$$\mathsf{S}_k[M] = \sum_{m=1}^{M} S\left[\hat{T}_k[m], m\right], 1 \le k \le \xi_M \qquad (4)$$

Since the actual HR trajectory should pass through the peaks in the spectra of different frames, the TS of the actual HR trajectory, in general, would be higher than other spurious trajectories. Hence, the frequency location index $(\hat{N}_M)$ corresponding to the estimated HR at the M-th frame is chosen to be the point of the unique trajectory which has the highest TS at the M-th frame. In other words $\hat{N}_M = \hat{T}_{k^\star}[M]$, where $k^\star = \arg\max_k \mathsf{S}_k[M]$.

For illustration, in Fig. 2, we consider a denoised PPG spectrogram up to M-th frame and the unique trajectories $(\mathcal{T}_{M-1})$ as inputs for MISPT algorithm. The black dots in the plots of the trajectories in $\mathcal{T}_{M-1}$ (Fig. 2(a)) indicate the points of initialization of the unique trajectories. The initialization at the M-th frame (blue solid circle) and the corresponding HR trajectory (red curve) obtained by the backward SPT are shown in Fig. 2(b). It should be noted that the initialization does not correspond to the ground-truth HR at the M-th frame (denoted by solid star in Fig. 2(b)). It is also seen that the HR trajectory with initialization at the M-th frame turns out to be a new trajectory (as shown in Fig. 2(c)) although the initialization point falls on one of the existing unique trajectories. This is because the trajectory formed by the backward SPT from an initial point may not match with the trajectory obtained from a forward SPT on which the initial point lies. Finally the frequency location index of the estimated HR, $\hat{N}_M$, for the denoised PPG spectrogram is shown by a red square in Fig. 2(d).

The HR in BPM is calculated from $\hat{N}_M$ using $BPM_{est}(M) = \frac{\hat{N}_M}{NFFT} \times Fs \times 60$, where Fs is the sampling rate of the PPG signal. It is important to note that the final HR estimate (red square) at the M-th frame is different from the frequency (blue solid circle) where the initialization is done. This indicates that the TS based HR estimate need not necessarily match with the highest peak of the spectrum in a frame resulting in a HR estimate robust to the residual MA components in the denoised PPG signal.

III. Experimental Results

A. Datasets

For the experiments in this paper, we have used the PPG signal from 515 nm wavelength pulse oximeter and 3 accelerometer signals from tri-axis accelerometer along with single channel ECG as discussed in [26]. Data was collected from 12 male subjects of yellow skin aged between 18 to 35 years. Pulse oximeter and accelerometer were embedded in a wrist band. ECG signal was acquired from wet electrodes pasted on the chest. Data from these 12 subjects constitute the 12 datasets used in this work. ECG signal was manually annotated for ground-truth which is used for evaluation. The annotations are averaged over 8 seconds window with a shift of 2 seconds. PPG, accelerometer and ECG signals are sampled (Fs) at 125 Hz.

Data was collected from the subjects during walking or running on treadmill with speeds 1-2 km/hour for 0.5 minute, 6-8 km/hour for 1 minute, 12-15 km/hour for another minute and then go back to rest in 2.5 minutes in the reverse order of speed. Subjects were requested to minimize their hand movements for first 2-3 seconds. After which they had to perform actions such as buttoning the shirt, wiping off sweat.

B. Experimental Settings

HR estimation is done for each 8 seconds window (1000 samples) with a shift of 2 seconds (250 samples). ANC filter order is set to 9. $NFFT$ is chosen as 8192. Initialization parameter (δ) is varied from 1 to 161[2] with a step of 1. The evaluation window (Δ_s) for SPT is chosen to be 20.

Absolute average error (AAE) between the annotation (BPM_{true}) and estimate (BPM_{est}) is used to evaluate the performance of the algorithm as in [11], [26].

$$AAE = \frac{1}{F}\sum_{f=1}^{F} |BPM_{est}(f) - BPM_{true}(f)| \qquad (5)$$

where F is the number of frames for which the HR is estimated. The standard deviation (SD) is computed over all the frames of 12 datasets.

Evaluation of the proposed HR estimation is done on 1768 frames of 12 datasets as done in [11]. In addition, we also report results after excluding few initial frames (i.e., over 1745 frames)

[2]Among various datasets, dataset8 has the highest number of frames = 160. Then $\delta = 161$ would correspond to SPT on all datasets.

TABLE I
AAE (IN BPM) FOR EACH DATASET USING THE PROPOSED MISPT BASED HR ESTIMATION AS WELL USING JOSS AND TROIKA. AVERAGE (SD) AAE OVER FRAMES OF ALL DATASETS IS ALSO REPORTED. BOLD ENTRY IN EACH COLUMN INDICATES THE LEAST AAE OBTAINED BY AN ALGORITHM ON THE RESPECTIVE DATASET. THE UNDERLINED ENTRY SHOWS THE LEAST AAE OVER THE ENTIRE DATASET

	Set 1	Set 2	Set 3	Set 4	Set 5	Set 6	Set 7	Set 8	Set 9	Set 10	Set 11	Set 12	**Average (SD)**
MISPT-25	1.53	2.08	1.30	1.01	0.74	0.97	0.72	0.46	0.42	4.28	0.88	0.69	***1.26 (2.90)***
MISPT-125	1.58	1.80	**0.58**	**0.99**	0.74	**0.93**	0.73	**0.45**	**0.41**	**3.60**	0.88	**0.68**	***1.11 (2.33)***
JOSS	**1.33**	**1.75**	1.47	1.48	**0.69**	1.32	**0.71**	0.56	0.49	3.81	**0.78**	1.04	***1.28 (2.61)***
TROIKA-25	2.87	2.75	1.91	2.25	1.69	3.16	1.72	1.83	1.58	4.00	1.96	3.33	***2.42 (2.47)***
TROIKA-125	2.29	2.19	2.00	2.15	2.01	2.76	1.67	1.93	1.86	4.70	1.72	2.84	***2.34 (-)***

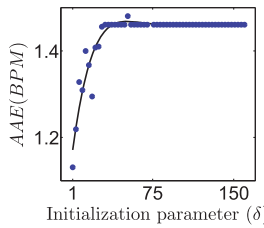

Fig. 3. Effect of Delta δ on AAE. The blue dots show the AAE averaged over 12 datasets for the respective δ. The black curve indicates the trend.

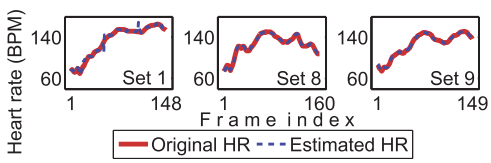

Fig. 4. Illustration of the original and estimated HR for three datasets.

of some datasets as done in [26]. The excluded frames correspond to the first 12 seconds of set 2, 8 seconds of set 3, 2 seconds of set 4, 2 seconds of set 8, 6 seconds of set 10 and 2 seconds of set 11. For comparison, we have used both TROIKA [11] as well as JOSS [26] algorithms.

C. Results and Discussion

Fig. 3 shows the change in the AAE with different values of δ. The AAE is averaged over all frames of 12 datasets. It is clear that decreasing δ reduces the AAE indicating that multiple initialization indeed helps in improving the HR estimate. It can be seen that SPT with single initialization ($\delta = 161$) results in an AAE of 1.46 BPM while MISPT with $\delta = 1$ results in an AAE of 1.11 BPM. From the plot it is also clear that the drop in AAE due to decreasing δ is not gradual. In fact, on an average, there is no drop in AAE for $\delta > 40$. As δ decreases below 40, a drop in AAE is observed with the least AAE for $\delta = 1$. It should be noted that $\delta = 1$ results in the least AAE consistently for all 12 datasets. Hence, all results are reported for $\delta = 1$ in this work. Fig. 4 shows the ground-truth and estimated HR for randomly chosen three datasets. It is clear that the ground-truth and estimated HR trajectories match well.

Listed in Table I are the AAE for each of the 12 datasets along with mean AAE and SD across frames of all datasets. Since results of JOSS were reported with PPG downsampled at 25 Hz, we also report the MISPT based results with PPG at 25 Hz. This is denoted by MISPT-25. For the MISPT on the 125 Hz PPG signal, the scheme is referred to as MISPT-125. Similarly, TROIKA-25 and TROIKA-125 refer to the TROIKA framework when applied to the PPG signal with 25 Hz and 125 Hz respectively.

It is clear that AAE over all frames of 12 datasets using MISPT-125 is lower than that using JOSS, TROIKA-25, and TROIKA-125 by 0.17, 1.31 and 1.23 BPM (absolute) respectively. These AAE reductions are 0.02, 1.16 and 1.08 BPM (absolute) when MISPT-25 is used indicating the better performance of MISPT over the state-of-the-art techniques. Comparison of AAE for each dataset shows that MISPT-125 achieves lower AAE for seven datasets (set 3, 4, 6, 8, 9, 10, 12) compared to JOSS. This is true for MISPT-25 too. When the initial few frames of some datasets are removed (as done in JOSS), the average (SD) AAE values over all datasets turn out to be 1.24 (2.90) and 1.10 (2.32) for MISPT-25 and MISPT-125 respectively suggesting further improvement over the JOSS performance. SD of MISPT-125 is less than all other algorithms which shows that HR estimates from MISPT-125 are closer to the manually annotated HR from the ECG signal compared to the state-of-the-art techniques.

IV. CONCLUSIONS

The proposed MISPT for HR monitoring uses an ANC filter for removing the MA in the PPG signal and combines multiple heart rate trajectories obtained by the SPT from multiple initializations to result in a better HR estimation accuracy compared to the state-of-the-art techniques. On an average, the MISPT based HR estimation takes 1.03 seconds (ranging from 0.94 seconds to 1.11 seconds)[3] for each of the 12 datasets, where each set is approximately 5 minutes long. Thus, the fast and accurate HR estimation using the proposed MISPT technique could potentially improve the quality of HR monitoring in wearable devices. It should be noted that the MISPT uses the signal information from the first to the current frame to compute the HR estimate at the current frame. However, for deploying MISPT for continuous monitoring of HR from the PPG data, spectrum of a fixed set of previous (buffer) frames can be used instead of the entire signal up to the current frame. Detailed investigation is required to determine the optimal buffer size. Investigation is also required to demonstrate the robustness of the proposed MISPT approach on data collected in free-living condition. It is known that the gait on treadmill is typically different from free walking [29]. However, the proposed approach does not exploit any pattern in the PPG or accelerometer data due to treadmill gait. Hence, it is expected that the performance of MISPT on data from free-living condition would be similar to the ones reported in this work.

[3]The runtime values are reported by executing MISPT using the MATLAB2014b in a desktop computer with Intel i7 64-bit processor and 8 Gb RAM.

REFERENCES

[1] N. Selvaraj, A. Jaryal, J. Santhosh, K. K. Deepak, and S. Anand, "Assessment of heart rate variability derived from finger-tip photoplethysmography as compared to electrocardiography," *J. Med. Eng. Technol.*, vol. 32, no. 6, pp. 479–484, 2008.

[2] C. L. Petersen, T. P. Chen, J. Mark Ansermino, and G. A. Dumont, "Design and evaluation of a low-cost smartphone pulse oximeter," *Sensors*, vol. 13, no. 12, pp. 16882–16893, 2013.

[3] Y. Mendelson and B. D. Ochs, "Noninvasive pulse oximetry utilizing skin reflectance photoplethysmography," *IEEE Trans. Biomed. Eng.*, vol. 35, no. 10, pp. 798–805, 1988.

[4] T. Tamura, Y. Maeda, M. Sekine, and M. Yoshida, "Wearable photoplethysmographic sensors - past and present," *Electronics*, vol. 3, no. 2, pp. 282–302, 2014.

[5] J. Lee, W. Jung, I. Kang, Y. Kim, and G. Lee, "Design of filter to reject motion artifact of pulse oximetry," *Comput. Stand. Interfaces*, vol. 26, no. 3, pp. 241–249, 2004.

[6] H. Han, M.-J. Kim, and J. Kim, "Development of real-time motion artifact reduction algorithm for a wearable photoplethysmography," in *29th Annu. Conf. IEEE Eng. Med. Biol.*, 2007, pp. 1538–1541.

[7] A. Garde, W. Karlen, J. M. Ansermino, and G. A. Dumont, "Estimating respiratory and heart rates from the correntropy spectral density of the photoplethysmogram," *PloS One*, vol. 9, no. 1, p. e86427, 2014.

[8] J. Yao and S. Warren, "A short study to assess the potential of independent component analysis for motion artifact separation in wearable pulse oximeter signals," in *27th Annu. Conf. IEEE Eng. Med. Biol.*, 2005, pp. 3585–3588.

[9] B. Kim and S. K. Yoo, "Motion artifact reduction in photoplethysmography using independent component analysis," *IEEE Trans. Biomed. Eng.*, vol. 53, no. 3, pp. 566–568, 2006.

[10] R. Krishnan, B. Natarajan, and S. Warren, "Two-stage approach for detection and reduction of motion artifacts in photoplethysmographic data," *IEEE Trans. Biomed. Eng.*, vol. 57, no. 8, pp. 1867–1876, 2010.

[11] Z. Zhang, Z. Pi, and B. Liu, "TROIKA: A general framework for heart rate monitoring using wrist-type photoplethysmographic signals during intensive physical exercise," *IEEE Trans. Biomed. Eng.*, vol. 62, no. 2, pp. 522–531, 2015.

[12] K. W. Chan and Y. T. Zhang, "Adaptive reduction of motion artifact from photoplethysmographic recordings using a variable step-size LMS filter," in *Proc. IEEE Sensors*, 2002, vol. 2, pp. 1343–1346.

[13] H. Han and J. Kim, "Artifacts in wearable photoplethysmographs during daily life motions and their reduction with least mean square based active noise cancellation method," *Comput. Biol. Med.*, vol. 42, no. 4, pp. 387–393, 2012.

[14] P. Wei, R. Guo, J. Zhang, and Y. T. Zhang, "A new wristband wearable sensor using adaptive reduction filter to reduce motion artifact," in *, Int. Conf. Information Technology and Applications in Biomedicine*, 2008, pp. 278–281.

[15] H. Fukushima, H. Kawanaka, M. S. Bhuiyan, and K. Oguri, "Estimating heart rate using wrist-type photoplethysmography and acceleration sensor while running," in *34th Annu. Conf. IEEE Eng. Med. Biol.*, 2012, pp. 2901–2904.

[16] L. B. Wood and H. H. Asada, "Active motion artifact reduction for wearable sensors using laguerre expansion and signal separation," in *27th Annu. Conf. IEEE Eng. Med. Biol.*, 2006, pp. 3571–3574.

[17] M. J. Hayes and P. R. Smith, "A new method for pulse oximetry possessing inherent insensitivity to artifact," *IEEE Trans. Biomed. Eng.*, vol. 48, no. 4, pp. 452–461, 2001.

[18] Y.-S. Yan, C. C. Y. Poon, and Y.-T. Zhang, "Reduction of motion artifact in pulse oximetry by smoothed pseudo wigner-ville distribution," *J. NeuroEng. Rehab.*, vol. 2, p. 3, 2005.

[19] M. Raghuram, K. Venu Madhav, E. H. Krishna, and K. A. Reddy, "Evaluation of wavelets for reduction of motion artifacts in photoplethysmographic signals," in *10th Int. Conf. Information Sciences Signal Processing and their Applications*, 2010, pp. 460–463.

[20] J. Y. A. Foo, "Comparison of wavelet transformation and adaptive filtering in restoring artefact-induced time-related measurement," *Biomed. Signal Process. Contr.*, vol. 1, no. 1, pp. 93–98, 2006.

[21] X. Sun, P. Yang, Y. Li, Z. Gao, and Y.-T. Zhang, "Robust heart beat detection from photoplethysmography interlaced with motion artifacts based on empirical mode decomposition," in *, Int. Conf. Biomedical and Health Informatics*, 2012, pp. 775–778.

[22] E. Pinheiro, O. Postolache, and P. Girão, "Empirical mode decomposition and principal component analysis implementation in processing non-invasive cardiovascular signals," *Measurement*, vol. 45, no. 2, pp. 175–181, 2012.

[23] B. Lee, J. Han, H. Jae Baek, J. Hyuk Shin, K. Suk Park, and W. Jin Yi, "Improved elimination of motion artifacts from a photoplethysmographic signal using a Kalman smoother with simultaneous accelerometry," *Physiol. Meas.*, vol. 31, no. 12, p. 1585, 2010.

[24] M. P. Tarvainen, S. D. Georgiadis, P. O. Ranta-aho, and P. A. Karjalainen, "Time-varying analysis of heart rate variability signals with a Kalman smoother algorithm," *Physiol. Meas.*, vol. 27, no. 3, p. 225, 2006.

[25] K. Nakajima, T. Tamura, and H. Miike, "Monitoring of heart and respiratory rates by photoplethysmography using a digital filtering technique," *Med. Eng. Phys.*, vol. 18, no. 5, pp. 365–372, 1996.

[26] Z. Zhang, "Photoplethysmography-based heart rate monitoring in physical activities via joint sparse spectrum reconstruction," *IEEE Trans. Biomed. Eng.*, 2015.

[27] B. Widrow, J. R. Glover Jr, J. M. McCool, J. Kaunitz, C. S. Williams, R. H. Hearn, J. R. Zeidler, E. Dong, Jr, and R. C. Goodlin, "Adaptive noise cancelling: Principles and applications," *Proc. IEEE*, vol. 63, no. 12, pp. 1692–1716, 1975.

[28] L. B. Wood and H. H. Asada, "Noise cancellation model validation for reduced motion artifact wearable PPG sensors using MEMS accelerometers," in *28th Annu. Conf. IEEE Eng. Med. Biol.*, 2006, pp. 3525–3528.

[29] C. Kirtley, *Clinical Gait Analysis: Theory and Practice*. Amsterdam, The Netherlands: Elsevier Health Sciences, 2006.

This paper previously published in IEEE Signal Processing Letters